

DSCC2017-5373

A GENERAL FRAMEWORK FOR MINIMIZING ENERGY CONSUMPTION OF SERIES ELASTIC ACTUATORS WITH REGENERATION

Edgar Bolívar^{1,2}, Siavash Rezazadeh², and Robert Gregg^{1,2}

Locomotor Control Systems Laboratory

¹ Department of Mechanical Engineering

² Department of Bioengineering

University of Texas at Dallas

Richardson, TX 75080, USA

Email: {edgarbolivar, siavash.rezazadeh, rgregg}@utdallas.edu

ABSTRACT

The use of actuators with inherent compliance, such as series elastic actuators (SEAs), has become traditional for robotic systems working in close contact with humans. SEAs can reduce the energy consumption for a given task compared to rigid actuators, but this reduction is highly dependent on the design of the SEA's elastic element. This design is often based on natural dynamics or a parameterized optimization, but both approaches have limitations. The natural dynamics approach cannot consider actuator constraints or arbitrary reference trajectories, and a parameterized elastic element can only be optimized within the given parameter space. In this work, we propose a solution to these limitations by formulating the design of the SEA's elastic element as a non-parametric convex optimization problem, which yields a globally optimal conservative elastic element while respecting actuator constraints. Convexity is proven for the case of an arbitrary periodic reference trajectory with a SEA capable of energy regeneration. We discuss the optimization results for the tasks defined by the human ankle motion during level-ground walking and the natural motion of a single mass-spring system with a nonlinear spring. For all these tasks, the designed SEA reduces energy consumption and satisfies the actuator's constraints.

1 INTRODUCTION

During the last two decades, research in soft robotics has revolutionized actuation for robotic systems [1]. Within the soft

robotics family, series elastic actuators (SEAs) demonstrate how elastic elements improve the functionality of prosthetic legs [2–4], humanoid robots [5], and manufacturing robots working in close contact with human users [6].

In contrast to rigid actuators, SEAs have an elastic element connected in series between the actuator and the load [7]. In general, the rigid actuator could be an electric motor, or a hydraulic or pneumatic cylinder. In this work, we only consider electric motors. When used in SEAs, they are normally connected to a high-ratio linear transmission, then an elastic element connects the transmission's output to the load. This architecture represents a typical implementation of SEAs [8]. Designs with a low ratio transmission are less common but still possible due to recent developments in high torque motors [9, 10].

SEA's architecture offers important benefits to the actuation of robotic systems, as shown in previous research. The elastic element in a SEA decouples the reflected inertia of the rigid actuator from the inertia of the load [5]. In addition, it can store mechanical energy and release it with enormous power. It also serves as a soft load cell, suitable for measuring and controlling force generation [11]. Robots using SEAs exploit these important characteristics in order to reduce the energy lost during impacts [5], increase the actuator's peak power [3], improve the safety of the human and robots [12], move loads with higher velocities [13], and/or reduce energy consumption of the system [14, 15].

How can an SEA reduce the energy consumption compared to rigid actuators? The answer is not intuitive, taking into account

that the elastic element cannot inject energy from an external source. As discussed in the initial developments of SEAs [16], the concept of natural dynamics provides a partial answer to this question. In this framework, energy consumption is minimized if the natural frequency of the elastic element matches the desired motion of the load. For instance, if the motion of the load is sinusoidal, it is possible to design an elastic element with constant stiffness that, once connected to the load, produces the required motion given an adequate initial elongation. In this ideal configuration the motor would stay still. In practice, however, the motor moves slightly to compensate for the energy lost due to heat and viscous friction generated by the elastic element and the load. As experimentally shown in [15, 17], this reduced motion of the motor consumes less energy than an electric motor driving the same load without an elastic element. This approach can generalize to more complex motion if nonlinear elastic elements are used. They are capable of multiple local natural frequencies based not only on their stiffness values and the inertia of the load, but also on the initial elongation and the displacement produced by the electric motor.

Although natural dynamics provide intuition about the possible benefits of elastic elements, there are many cases where the optimal choice of elastic element is not so obvious. For instance, the desired motion of the load may not correspond to the natural frequency of a conservative elastic element. Even if the required motion matches a natural frequency of oscillation, holding the motor's initial position dissipates energy by Joule heating (i.e., copper losses) if the system is backdrivable. For this configuration, a more accurate formulation considers the natural frequency of the double-mass spring system formed by the elastic element, the motor, and load inertia. Note that the natural frequency of this system may not have an analytic solution once nonlinear elastic elements are considered. Natural dynamics also do not explain how to design the elastic element in the presence of actuator constraints. Maximum deflection of the elastic element, maximum torque, and maximum velocity of the motor are typical constraints imposed by the construction of the device.

Computing the energy cost associated with different elastic elements is a common alternative to the natural dynamics methodology. This approach parameterizes the behavior of the elastic element and evaluates the energy consumption across values of the parameters. For instance, if the elastic element is defined as a linear spring, then its stiffness is the optimization parameter [2]. In contrast to natural dynamics, constraints can be included explicitly in the optimization problem. However, this method can only guarantee a minimum value within the scope of the parameter's grid, but it may not be a global solution. It is also computationally expensive to evaluate all the points in a dense grid of the parameter space. This becomes problematic once multiple degrees of freedom are considered. In addition, assuming a specific shape for the elastic element function limits the elastic elements that can be considered. For instance, it is possible that a non-

linear conservative spring could reduce the energy consumption further compared to a parameterized linear spring. Because of these limitations, the design of elastic elements that reduce energy consumption for SEAs remains an open question.

Our contribution

In this paper the elastic element is defined, in the most general conservative form, as the function

$$\tau_{\text{ela}} = f(\delta), \quad (1)$$

where δ is the elongation and τ_{ela} the torque of the elastic element. Our contribution is to specify $f(\delta)$ as the optimal solution of a convex quadratically constrained quadratic program (convex-QCQP) subject to actuator constraints. We constrain $f(\delta)$ to be any monotonically increasing function to ensure that it represents a conservative elastic element. In contrast to previous methods, we do not assume a specific parameterization of $f(\delta)$ or that the reference motion of the load resembles natural dynamics. As a result, our method identifies the optimal elastic element, linear or nonlinear, that minimizes energy consumption for backdrivable SEAs following arbitrary periodic trajectories subject to actuator constraints. Using this optimization tool, we show how motor inertia, transmission ratio, and non-linearity of the elastic element affect energy consumption.

The content is organized as follows. A description of the energy flow and modeling of an SEA is provided in Sec. 2. This technical introduction will be used to formulate the design of an elastic element as a convex optimization problem in Sec. 3. Simulation examples with multiple reference trajectories are analyzed in Sec. 4, followed by conclusions.

2 SYSTEM DESCRIPTION AND MODELING

SEAs are mechatronic devices that transduce electrical energy into mechanical and vice versa. From the energy perspective, they are similar to traditional electric motors; however, their capability to store and release elastic energy creates an additional opportunity to reduce their energy consumption. This section describes the energy flow of SEAs as an initial step of our formulation.

In this work, we analyze SEAs powered by a battery and an electric motor, a typical scenario for a wearable robot. The corresponding energy flow and main components are illustrated in Fig. 1. In practice, every component in the system is capable of dissipating energy. For example, the battery self-discharges, the motor drive produces Joule heat, friction in the transmission generates heat, and the elastic elements are not purely elastic (i.e., dissipate energy through their viscous behavior). We will concentrate on the energy consumed by the motor since it is the largest consumption in the system.

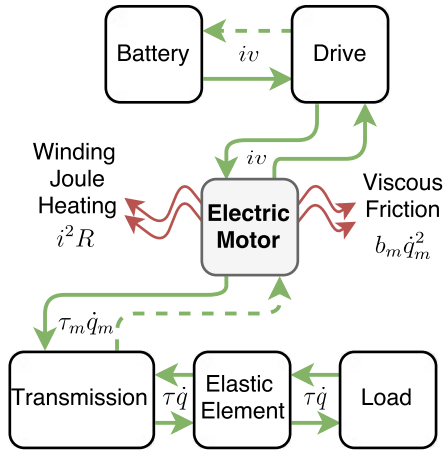


FIGURE 1. Energy flow of an SEA: Dashed lines indicate that the energy path may or may not exist depending on the construction of the device. For instance, energy flowing from the drive to the battery requires drivers capable of regeneration. Energy flowing from the transmission to the electric motor requires the motor-transmission system to be backdrivable.

Energy flow in an electric motor occurs in two principal modes of operation: actuator and generator mode. As an actuator, the electric motor receives electrical energy from the battery/driver and converts it into mechanical energy and heat. Traditional motor drives and mechanical transmissions are designed so that the electric motor can always operate in this mode. A more interesting scenario occurs when the motor is also allowed to work as a generator. Suppose the motor is decelerating the load. In this case, the energy of the load and elastic element move the actuator's rotor and generate electrical energy to be stored in the battery.

However, traditional SEAs may not function in generator mode. These designs typically have linear transmissions with high reduction ratios. The reflected inertia of the motor after the transmission, which is proportional to the reduction ratio squared, is normally very high compared to the load. For example, three recent SEA designs reflect output inertia of 360 kg, 270 kg, and 294 kg for the UT-SEA [8], Valkyrie's SEA [18], and THOR-SEA [19] respectively, as indicated by [10]. As a consequence, the system requires a high load to backdrive. If the system is not backdrivable, no electric energy can be recovered from the motion of the load. An additional but less common limitation is the motor driver. In order to regenerate energy, motor drivers should be selected such that the electrical energy recovered from the motion of the rotor can flow back to charge the battery.

In this work, we assume the SEA has been designed such that energy can flow from the load to the energy source and vice versa.

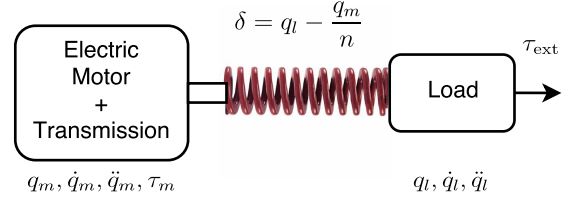


FIGURE 2. Diagram of a SEA. Eqns. 3-4 illustrate the system's equations of motion.

In other words, it is backdrivable and adequate electronics allow energy to flow to and from the battery. In this case, the energy it consumes, E_m , is given by

$$E_m = \int_{t_0}^{t_f} \underbrace{\frac{\tau_m^2}{k_m^2}}_{\text{Winding Joule heating}} + \underbrace{\tau_m \dot{q}_m}_{\text{Rotor mechanical power}} dt, \quad (2)$$

where t_0 and t_f are the initial and final times of the trajectory respectively, k_m is the motor constant, τ_m the torque produced by the motor, and \dot{q}_m the motor's angular velocity. Notice that energy associated with Joule heating can be also written as $i_m^2 R$, since $\tau_m = i_m k_{mt}$ and $k_m = k_{mt} / \sqrt{R}$, where i_m is the electric current flowing through the motor, R the motor terminal resistance, and k_{mt} the motor torque constant. As a comparison, consider the case where the motor driver does not regenerate energy. In this case, the rotor mechanical power would be expressed as $\max(\tau_m \dot{q}_m, 0)$ instead of $\tau_m \dot{q}_m$, in Eqn. 2, meaning that the motor only consumes energy. When the motor acts as a generator, the energy it converts does not transfer to the battery but instead dissipates as heat through the motor driver electronics.

Figure 2 illustrates the configuration of an SEA. Using the Newton-Euler method, the corresponding balance of torques at the motor and load side provides the following equations of motion

$$I_m \ddot{q}_m = -b_m \dot{q}_m + \tau_m + \frac{\tau_{\text{ela}}}{\eta r}, \quad (3)$$

$$\tau_{\text{ela}} = g(q_l, \dot{q}_l, \ddot{q}_l, \tau_{\text{ext}}), \quad (4)$$

where I_m is the inertia of the motor, b_m its viscous friction coefficient, τ_{ela} the torque produced by the elastic element, r the transmission ratio, η the efficiency of the transmission, and $g(q_l, \dot{q}_l, \ddot{q}_l, \tau_{\text{ext}})$ defines the load dynamics as a function of the corresponding load position q_l , load velocity \dot{q}_l , load acceleration \ddot{q}_l , and the external torque applied to the load τ_{ext} . For instance, in the case of an inertial load with viscous friction the load dynamics

are defined by

$$g(q_l, \dot{q}_l, \ddot{q}_l, \tau_{\text{ext}}) = -I_l \ddot{q}_l + b_l \dot{q}_l, \quad (5)$$

where I_l is the inertia of the load, and b_l its corresponding viscous friction coefficient. The elongation of the elastic element is defined as

$$\delta = q_l - \frac{q_m}{r}. \quad (6)$$

As seen in Eqns. 3-4, the elastic element cannot modify the torque required to perform the motion, τ_{ela} , but it can modify the position of the motor such that $I_m \ddot{q}_m + b_m \dot{q}_m$ reduces the torque of the motor, τ_m .

If periodic motion is considered, τ_m from Eqn. 3 can be replaced in the expressions of energy, Eqn. 2, to make the following simplification

$$\begin{aligned} \int_{t_0}^{t_f} \tau_m \dot{q}_m dt &= \int_{t_0}^{t_f} \left(I_m \ddot{q}_m + b_m \dot{q}_m - \frac{\tau_{\text{ela}}}{\eta r} \right) \dot{q}_m dt, \\ &= \int_{t_0}^{t_f} \left(b_m \dot{q}_m^2 - \frac{\tau_{\text{ela}} \dot{q}_m}{\eta r} \right) dt + \int_{t_0}^{t_f} I_m \dot{q}_m \frac{d\dot{q}_m}{dt} dt, \\ &= \int_{t_0}^{t_f} \left(b_m \dot{q}_m^2 - \frac{\tau_{\text{ela}} \dot{q}_m}{\eta r} \right) dt + \int_{\dot{q}_{m0}}^{\dot{q}_{mf}} I_m \dot{q}_m d\dot{q}_m, \\ &= \int_{t_0}^{t_f} \left(b_m \dot{q}_m^2 - \frac{\tau_{\text{ela}}}{\eta r} (\dot{q}_m - r\dot{q}_l + r\dot{q}_l) \right) dt, \\ &= \int_{t_0}^{t_f} \left(b_m \dot{q}_m^2 + \frac{\tau_{\text{ela}} \dot{q}_l}{\eta} \right) dt - \int_{\delta_0}^{\delta_f} \frac{\tau_{\text{ela}}}{\eta} d\delta, \\ &= \int_{t_0}^{t_f} \left(b_m \dot{q}_m^2 + \frac{\tau_{\text{ela}} \dot{q}_l}{\eta} \right) dt, \end{aligned} \quad (7)$$

for periodic motion, $\dot{q}_{mf} = \dot{q}_{m0}$, and $\delta_f = \delta_0$. This simplification illustrates two concepts. First, the energy associated with the inertia of the motor is zero for periodic motion. This will be useful to show convexity of the optimization problem. Second, the mechanical energy provided to or absorbed from the motion of the load (i.e., $\int_{t_0}^{t_f} \frac{\tau_{\text{ela}} \dot{q}_l}{\eta} dt$) will be provided or absorbed by the electric motor regardless of the elastic element.

3 STIFFNESS DESIGN AS A CONVEX OPTIMIZATION PROBLEM

In this section, the elastic element will be defined such that it minimizes the energy consumption of the motor for a given

task. Specifically, the optimization will define the function $f(\delta)$ in Eqn. 1 such that the expression in Eqn. 2 is minimized and satisfies specific constraints. In simple terms, this is equivalent to

$$\begin{aligned} &\text{minimize}_{f(\delta)} \quad \mathbf{Energy\ consumed\ by\ the\ motor,} \\ &\text{subject to} \quad \mathbf{Dynamics\ of\ the\ system,} \\ &\quad \quad \quad \mathbf{Actuator\ constraints.} \end{aligned}$$

In this work, the given task is defined as a reference trajectory $q_{l\text{ref}}(t)$, its corresponding time derivatives $\dot{q}_{l\text{ref}}(t)$, $\ddot{q}_{l\text{ref}}(t)$, and the external torque $\tau_{\text{ext}}(t)$. In order to draw conclusions independent of the controller design, we will assume perfect tracking, i.e. $q_l(t) \equiv q_{l\text{ref}}(t)$, $\dot{q}_l(t) \equiv \dot{q}_{l\text{ref}}(t)$, and $\ddot{q}_l(t) \equiv \ddot{q}_{l\text{ref}}(t)$.

Dynamics of the system

Equations (3-4) illustrate the dynamics of the system. They consider continuous time derivatives of q_m . In order to formulate this in a convex optimization framework, we approximate the continuous time derivative with a discrete time representation. This can be expressed as the following matrix operation $\dot{\hat{q}}_m \approx D \hat{q}_m$, where $\hat{q}_m, \dot{\hat{q}}_m \in \mathbb{R}^n$ is the discrete representation of q_m and \dot{q}_m , n the number of samples, $D \in \mathbb{R}^{n \times n}$ is defined as

$$D = \begin{bmatrix} 0 & 1 & 0 & 0 & \dots & -1 \\ -1 & 0 & 1 & 0 & \dots & 0 \\ \vdots & \ddots & & & & \vdots \\ 0 & \dots & -1 & 0 & 1 & \\ 1 & \dots & & -1 & 0 & \end{bmatrix} \frac{1}{2\Delta t}, \quad (8)$$

and Δt is the sample rate. $D \hat{q}_m$ is the discrete time derivative of \hat{q}_m , based on the central difference method, a similar definition of D can be done for trajectories with variable sample rates. For the sake of this analysis, we assume a fixed sample time without loss of generality. The first and last rows of D assume that \hat{q}_m represents a periodic trajectory, i.e. $\hat{q}_m(n+1) = \hat{q}_m(1)$. Then the equations of motion, Eqns. 3-4, can be approximated as

$$\hat{\tau}_m = (I_m D D + b_m D) \hat{q}_m - \hat{\tau}_{\text{ela}} \frac{1}{\eta r}, \quad (9)$$

$$\hat{\tau}_{\text{ela}} = \hat{g}(\hat{q}_l, \hat{\dot{q}}_l, \hat{\ddot{q}}_l, \hat{\tau}_{\text{ext}}), \quad (10)$$

$$\hat{\delta} = \hat{q}_l - \hat{q}_m \frac{1}{r}, \quad (11)$$

where $\hat{\tau}_m, \hat{\tau}_{\text{ela}}, \hat{q}_l, \hat{\dot{q}}_l, \hat{\ddot{q}}_l, \hat{\tau}_{\text{ext}} \in \mathbb{R}^n$ represent the discrete sampled versions of the motor torque, torque of the elastic element, load position, load velocity, load acceleration, and external torque applied to the load, respectively.

The objective in our optimization is to define the elastic element, which is equivalent to finding the function $f(\delta)$. The function $g(\cdot)$ defines the required values of torque of the elastic element given a reference trajectory but it does not relate them with the elongation of the elastic element. The optimization is then focused on the relationship of the given τ_{ela} and the elongation δ . Since the elongation is partially defined by the reference load position, Eqn. 11, the optimization problem can be interpreted as finding the position of the motor, q_m , such that the energy consumption of the motor is minimized. Once the position of the motor is established, the deflection of the elastic element is defined and can be used in conjunction with the given τ_{ela} to generate $f(\delta)$.

Cost function: Energy consumed by the motor

Based on the discrete formulation of the dynamics, Eqns. 9-11, the energy required by the motor, Eqn. 2, can be approximated in discrete form as

$$\begin{aligned} E_m &\approx \sum_{i=1}^n \left(\frac{\hat{\tau}_{m_i}^2}{k_m^2} + \hat{\tau}_{m_i} \hat{q}_{m_i} \right) \Delta t, \\ &= \left(\frac{\hat{\tau}_m^T \hat{\tau}_m}{k_m^2} + \hat{\tau}_m^T D \hat{q}_m \right) \Delta t. \end{aligned} \quad (12)$$

Actuator constraints

The definition of the elastic element relies on the definition of $f(\delta)$. For conservative elastic elements, the function $f(\delta)$ imposes two specific constraints. First, $f(\delta)$ is a function that lies on the I and III quadrants of the torque-elongation Cartesian frame. Considering elongation and torque as the corresponding input and output of the elastic element, this implies that it is a passive system. Second, we consider that the function $f(\delta)$ is bijective, a given elongation produces a unique torque and a given torque is being produced by a unique elongation.

These two constraints can be expressed mathematically as set of equality and inequality constraints. Specifically, we define the vector α_1 to constraint $f(\delta)$ to lie in the I and III quadrants of the torque-elongation Cartesian frame. The vector α_2 will indicate that a given torque is generated by a unique elongation. Recall that the torque of the elastic element is a constant vector given from the reference trajectory, Eqn. 4. The inequality and equality constraints are

$$\alpha_1 \leq 0, \quad (13)$$

$$\alpha_2 = 0, \quad (14)$$

where

$$\begin{aligned} \alpha_{1_i} &:= \begin{cases} -\hat{\delta}_i & \text{if } \hat{\tau}_{\text{ela}_i} \geq 0 \\ \hat{\delta}_i & \text{if } \hat{\tau}_{\text{ela}_i} < 0 \end{cases}, \quad i = 1, \dots, n, \\ \alpha_{2_j} &:= \hat{\delta}_i - \hat{\delta}_j \text{ if } \hat{\tau}_{\text{ela}_i} = \hat{\tau}_{\text{ela}_j}, \quad i, j = 1, \dots, n, \end{aligned} \quad (15)$$

and l is the number of times that $\hat{\tau}_{\text{ela}_i} = \hat{\tau}_{\text{ela}_j}$. In addition to these constraints, traditional actuator constraints such as maximum elongation of the elastic element, maximum and minimum torque of the motor, as well as bounds on the motor velocity are considered in our formulation.

The optimization problem

The optimization problem is then written in discrete form as

$$\begin{aligned} &\text{minimize}_{\hat{q}_m} \quad \left(\frac{\hat{\tau}_m^T \hat{\tau}_m}{k_m^2} + \hat{\tau}_m^T D \hat{q}_m \right) \Delta t, \\ &\text{subject to} \\ &\quad \hat{\tau}_m = (I_m D D + b_m D) \hat{q}_m - \hat{\tau}_{\text{ela}} \frac{1}{\eta r}, \\ &\quad \|\hat{\tau}_m\|_{\infty} \leq \tau_{\text{max}}, \\ &\quad \|D \hat{q}_m\|_{\infty} \leq \dot{q}_{\text{max}}, \\ &\quad \|\hat{\delta}_m\|_{\infty} \leq \delta_{\text{max}}, \\ &\quad \alpha_1 \leq 0, \\ &\quad \alpha_2 = 0, \end{aligned} \quad (16)$$

where δ_{max} , τ_{max} , \dot{q}_{max} , are the corresponding maximum values for the elongation of the elastic element, torque, and velocity of the motor respectively. Inequality and equality for vectors are considered to be componentwise.

Convexity of the optimization problem

The optimization problem in Eqn. 16 is convex if the cost is a convex function and the constraints represent a convex set of the optimization variable, \hat{q}_m , [20]. We use the fact that the sum of two convex functions is a convex function to analyze each term in Eqn. 12, [20]. Using the definition of torque from the discrete dynamics, Eqn. 9, the cost associated with winding Joule heating can be written as

$$\frac{\hat{\tau}_m^T \hat{\tau}_m}{k_m^2} \Delta t = \frac{\Delta t}{k_m^2} (\hat{q}_m^T A^T A \hat{q}_m + 2\beta A \hat{q}_m + \beta^T \beta), \quad (17)$$

where

$$A := (I_m DD + b_m D),$$

$$\beta := -\hat{\tau}_{\text{ela}} \frac{1}{\eta r}.$$

The Hessian of the quadratic function in Eqn. 17, $\left(\frac{\partial^2}{\partial^2 q_{md}} \frac{\hat{v}_{md}^T \hat{v}_{md}}{k_m^2} \Delta t\right) = A^T A$, is the Gramian matrix of A . This is a positive semi-definite matrix, as can be seen from its singular value decomposition. This shows that the quadratic equation is convex with respect to \hat{q}_m .

The cost associated with the mechanical energy of the rotor can be analyzed in a similar manner; however, an important distinction will be made for periodic and non periodic motion. Using the simplified expression for the mechanical energy of the motor, Eqn. 7, this cost can be written as

$$\begin{aligned} \hat{\tau}_m^T D \hat{q}_m \Delta t &= (A \hat{q}_m + \beta)^T D \hat{q}_m \Delta t, \\ &= b_m \hat{q}_m^T D^T D \hat{q}_m \Delta t + \beta^T D \hat{q}_m \Delta t. \end{aligned} \quad (18)$$

Then, convexity can be shown in a similar manner as before: the Hessian of the quadratic equation, Eqn. 18, is $D^T D$, which is the positive semi-definite Gramian matrix of D . If the reference motion is not periodic, then the objective function is in general not convex, the eigenvalues of the matrix $A^T D$ can be positive or negative. However, the problem can be formulated as a non-convex QCQP [21]. For this, note that $\hat{q}_m^T A^T D \hat{q}_m = \frac{1}{2} \hat{q}_m^T (A^T D + D^T A) \hat{q}_m$. Defining the symmetric matrix $B = \frac{1}{2} (A^T D + D^T A)$, we rewrite Eqn. 18 as

$$\hat{\tau}_m^T D \hat{q}_m \Delta t = \hat{q}_m^T B \hat{q}_m \Delta t + \beta^T D \hat{q}_m \Delta t. \quad (19)$$

With this analysis we conclude that the cost function in Eqn. 16 is convex for periodic motion and is non-convex quadratic for non-periodic motion.

Once the constraints in Eqn. 16 are written with respect to \hat{q}_m , they define a set of inequality and equality constraints of the form $C \hat{q}_m \leq d$ and $P \hat{q}_m = r$, where $C, P \in \mathbb{R}^{n \times n}$ and $d, r \in \mathbb{R}^n$. These constraints represent a convex set of \hat{q}_m , as seen in [20], which are equivalent to a polyhedra.

4 EXAMPLE CASES

In this section, we solve the optimization problem in Eqn. 16 to define the SEA's elastic element for two different reference trajectories: natural oscillation of a nonlinear spring, and motion of the ankle during level ground human walking. For each case, the trajectory of the load (i.e., $q_l, \dot{q}_l, \ddot{q}_l$, and τ_{ext} in Eqn. 4) is given

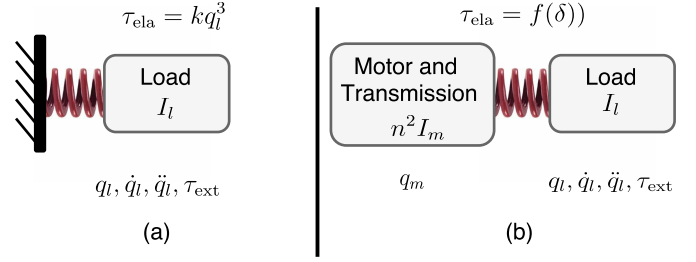


FIGURE 3. (a) Single mass-spring system. The elastic element describes the nonlinear spring with $\tau_e = kq_l^3$. (b) Double mass-spring system. The equilibrium position of the elastic element is $q_l = q_m/r$, elongation is defined as $\delta = q_l - q_m/r$. Motor and transmission are considered to be backdrivable.

and the optimization problem is numerically solved using CVX, a package for specifying and solving convex programs [22, 23]. In all simulations, CVX executed the solver Mosek [24] with precision settings `cvx_precision best`.

We used the parameters of a commercial frameless motor (Model: ILM 85x26, RoboDrive, Seefeld, Germany), for the task representing the natural oscillation of a nonlinear spring. This motor has a high nominal and peak torque, requiring a lower reduction ratio. This configuration favors backdrivability of the SEA. For the motion of the ankle, we used the parameters of the motor (Model: EC30, Maxon motor, Sachseln, Switzerland) and transmission used in the ankle joint actuator of the powered prosthetic leg designed and build at the University of Texas at Dallas (UTD) [25]. The parameters of the two systems are summarized in Table 1.

Natural oscillation of a nonlinear spring

Figure 3-(a) describes a single mass-spring system with a nonlinear spring, $\tau_{\text{ela}} = \alpha q_l^3$, and corresponding equation of motion $\tau_{\text{ela}} = -I_l \ddot{q}_l$, where $I_l = 125 \text{ gm}^2$ is the inertia of the load and $\alpha = 40 \text{ Nm/rad}^3$. No actuator constraints are considered for this trajectory. Given an initial displacement, $q_l(0) = \pi/2 \text{ rad}$, the position of the load will oscillate as shown in Fig. 4. This natural vibration is defined as our reference motion.

For analysis, we solve the optimization problem for the system in Fig. 3-(b), which represents an SEA driving the same inertial load as in Fig. 3-(a). The SEA can generate the reference motion with the motor holding its initial position if the elastic element matches the nonlinear spring in Fig. 3-(a), i.e., $\tau_{\text{ela}} = \alpha \delta^3$. However, this approach may not be energetically efficient. If the system is backdrivable, the motor must apply a reactionary torque to hold its initial position. This torque requires a current that generates heat losses at the motor's winding due to Joule heating. In contrast, we can solve the optimization problem in Eqn. 16 to find

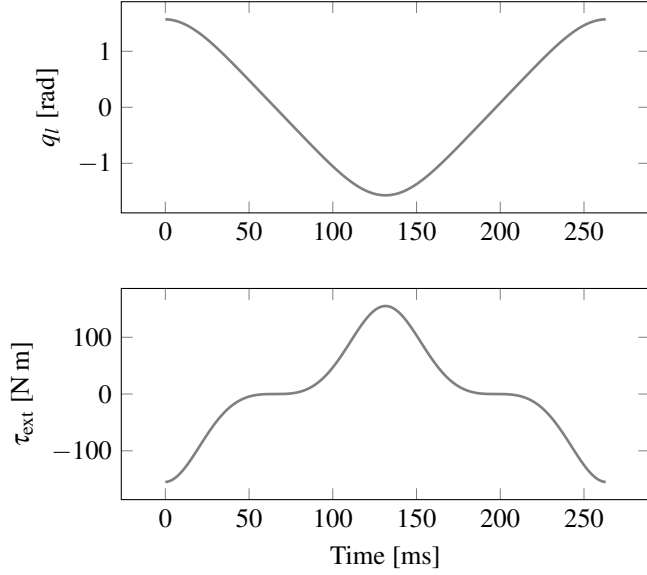


FIGURE 4. The reference trajectory of the load is defined by the natural oscillation of the single mass-spring system in Fig. 3-(a) with $\alpha = 40 \text{ Nm/rad}^3$, $I_l = 125 \text{ gm}^2$, and $q_l(0) = \pi/2 \text{ rad}$.

TABLE 1. Simulation parameters based on the motor ILM85x26 from RoboDrive and EC30 from Maxon motor.

Parameter	ILM85 x26	EC30	Units
Motor torque constant, k_t	0.24	0.0136	N m/A
Motor terminal resistance, R	323	102	m Ω
Rotor inertia, I_{mr}	1.15	0.0333	kgcm ²
Rotor assembly, I_{ma}	0.131	0	kgcm ²
Motor inertia, $I_m = I_{mr} + I_{ma}$	1.246	0.0333	kgcm ²
Gear ratio, r	22	720	
Efficiency transmission, η	1	1	
Motor viscous friction, b_m	60	6.66	$\mu\text{N m s/rad}$

the elastic element that minimizes the total energy expenditure (i.e., winding losses and viscous friction). In order to evaluate the performance of the proposed methodology, we solve the problem in Eqn. 3 to minimize three different cost functions: the energy dissipated by winding Joule heating, the energy dissipated by viscous friction, or the total energy consumption. The resulting elastic elements, torques, and positions of the motor are illustrated in Fig. 5. Table 2 summarizes the energy balance.

Minimizing viscous friction leads to the same elastic element as in Fig. 3-(a). The energy required to produce the motion is then 20.174 J which is all dissipated in the motor's winding. In

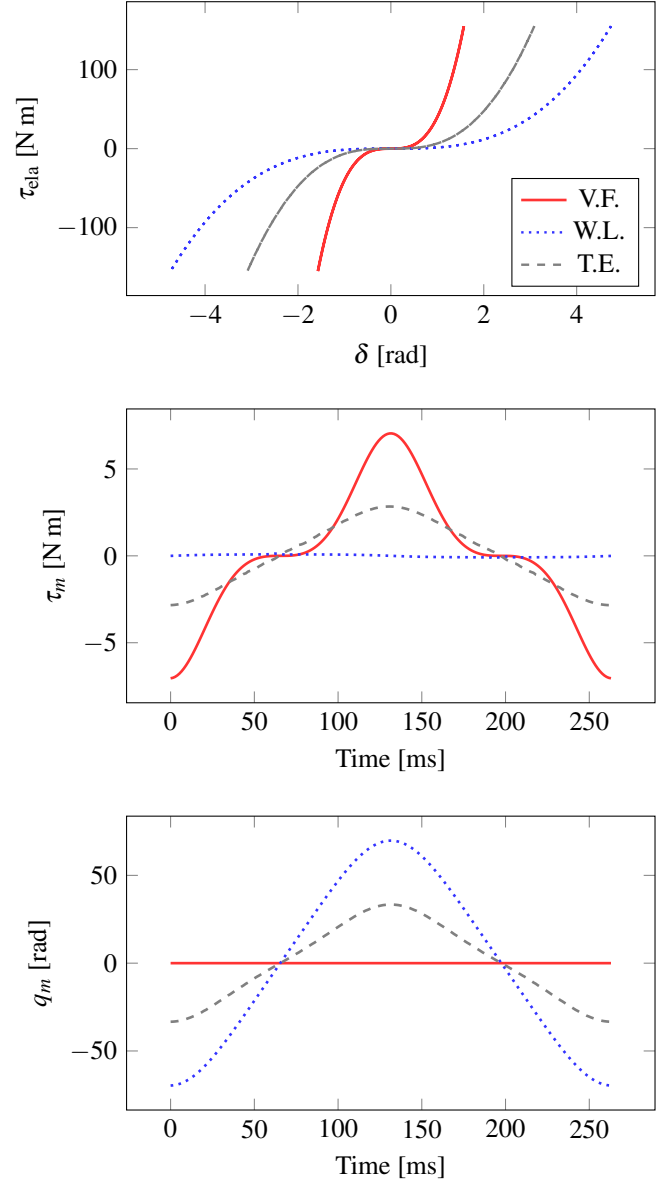


FIGURE 5. Optimization results considering natural oscillation of a nonlinear spring as the reference motion. The solid line corresponds to the elastic element that minimizes the energy consumption due to viscous friction (VF). It matches $\tau_{\text{ela}} = \alpha\delta^3$, the nonlinear spring used in the single mass-spring system. The dotted line describes the elastic element that minimizes winding losses (WL) due to Joule heating. The dashed line describes the elastic element that minimizes both winding losses and viscous friction, i.e., total energy (TE). The corresponding energy expenditure is shown in Table 2.

contrast, minimizing the total energy consumption results in a cost of 9.66 J; 52% less compared to the previous case. The elastic element is nonlinear but is not defined by $\tau_{\text{ela}} = 40\delta^3$ and the

TABLE 2. Energy expenditure with different cost functions. V.F. is the cost associated with viscous friction, W.L. winding losses due to Joule heating, and T.E. is the total energy consumption. As a comparison a motor without elastic element will consume 50.101 J for the same trajectory.

Cost function	Energy dissipated by Joule heating [J]	Energy dissipated by viscous friction [J]	Total Energy expenditure [J]
V.F.	20.174	0	20.174
W.L.	0.007	20.759	20.766
T.E.	5.099	4.558	9.657

TABLE 3. Actuator constraints as defined in Eqn. 16.

Constraint	Value	Units
Maximum motor peak torque, τ_{\min}	283.8	mN m
Maximum motor angular velocity, \dot{q}_{\max}	20000	rpm
Maximum elastic element elongation, δ_{\max}	$\pi/6$	rad

motor no longer remains stationary. Minimizing only the energy dissipated by the motor's winding leads to an elastic element that requires almost no torque for the electric motor, as seen in Fig. 5. This elastic element approximates the natural dynamics of the double mass-spring system defined by the inertia of the load and the motor; however, due to viscous friction the energy required increases to 20.766 J. In conclusion, minimizing the total energy expenditure leads to the lower consumption. It provides the best balance between the energy dissipated by Joule heating and viscous friction.

Human level ground walking. The ankle joint

One important advantage of our methodology is the ability to analyze arbitrary periodic trajectories. In this section, the reference motion (i.e., $q_l, \dot{q}_l, \ddot{q}_l$, and τ_{ext}) is defined by the kinematics and kinetics of the human ankle during level ground walking, as described in [26]. In particular, we analyze the ankle trajectories for slow, normal, and fast walking speeds and three subject weights: 65, 75, and 85 kg. These reference trajectories are shown in Fig. 6. Actuator constraints for the optimization problem are defined in Table 3.

The optimal elastic elements along with the torques and positions of the motor are illustrated in Fig. 7. As shown in Eqn. 7, the energy of the load (i.e., $\int_{t_0}^{t_f} \frac{\tau_{\text{ela}} \dot{q}_l}{\eta} dt$) is always provided by the motor regardless of the SEA's elastic element. Therefore,

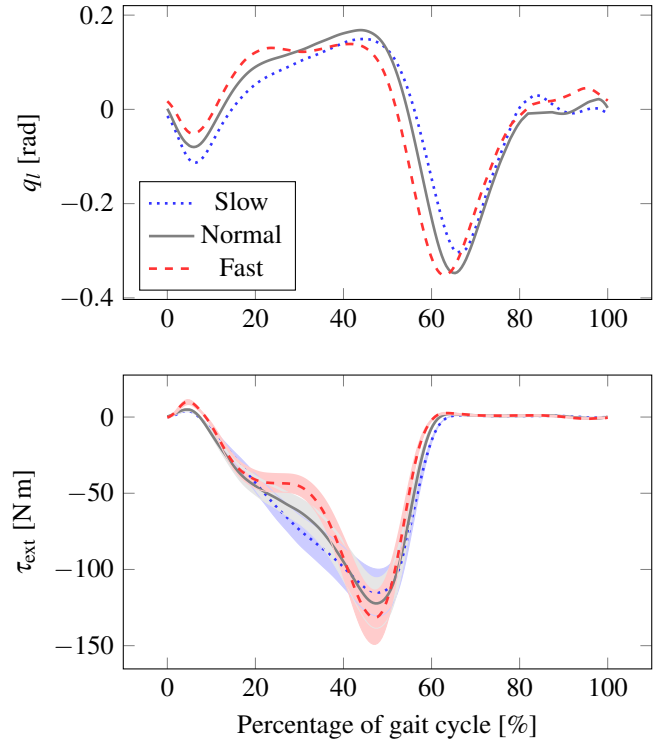


FIGURE 6. Motion of the human ankle during level ground walking as shown in [26]. Slow, normal, and fast walking speeds are equivalent to cadences of 87, 105, and 123 steps per minute. The gait cycle begins with heel contact of one foot and finishes with the subsequent occurrence of the same foot [26]. In average, the ankle of a 75 kg subject walking at normal speed provides about 17 J during a single gait cycle. In the lower figure, translucent regions denote the minimum and maximum external torques corresponding to 65 kg and 85 kg subjects.

energy savings for an SEA will be considered as the reduction of dissipated energy between a rigid motor without elastic element and an SEA. For example, during normal speed the ankle of a 75 kg subject provides about 17 J per stride; however, the EC30 motor with the characteristics described in Table 1, without an elastic element, requires 33 J. The extra 16 J are dissipated in the motor's winding by Joule heating and viscous friction. In contrast, the same motor connected in series with our optimal elastic element requires about 25 J per stride. The energy dissipated will be 8 J, a reduction of about 50% compared to a motor without an elastic element. A similar analysis for different walking speeds and subject weights is summarized in Fig. 8. Energy reduction is shown for all the cases considered. The optimal elastic element is nonlinear as shown in Fig. 7. This indicates that, for the given electric motor and transmission, a quadratic elastic element would be the most efficient to generate the ankle motion. Manufacturing of this nonlinear elastic element can be achieved using design methodologies such as [27].

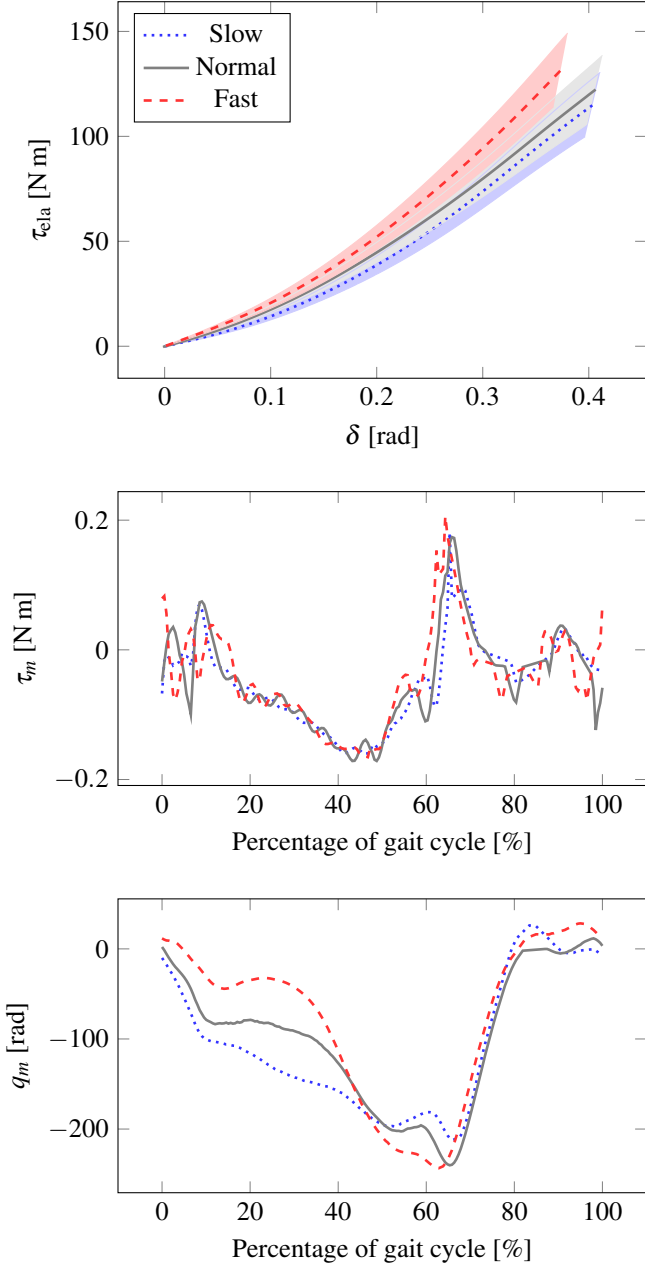


FIGURE 7. Optimization results considering motion of the ankle as the reference trajectory. Dotted, solid, and dashed lines indicate results for slow, normal, and fast level-ground walking speeds, respectively. Translucent regions denote upper and lower bounds corresponding to 85 kg and 65 kg subjects.

5 CONCLUSION

The proposed methodology reduced energy in all the cases, but the amount of energy saved should be analyzed in an individual basis depending on the reference motion and mechanical

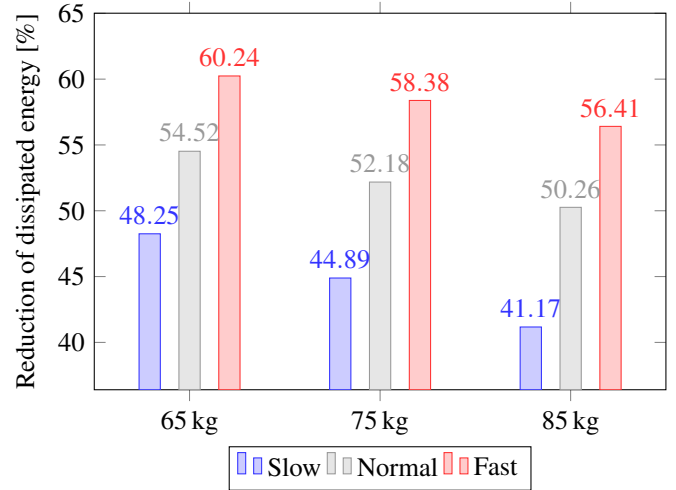


FIGURE 8. Energy savings for the ankle reference trajectory. Results for slow, normal, and fast level-ground walking for three different subject's weights.

configuration of the device. The inertia, torque constant, terminal resistance, and viscous friction coefficient of the motor as well as the transmission ratio played an important role in the amount of energy that the elastic element could reduce. For instance, the ankle trajectory was also analyzed using the RoboDrive's motor. Including actuator constraints, the elastic element could reduce only 2.65% of the energy dissipated. Neglecting actuator constraints could reduce 6.75% instead. This indicates as well the importance of actuator constraints on the design of the elastic element.

Notice that using an elastic element to save energy can decrease or increase the peak power of the motor. Actuator constraints in the optimization guarantee that the peak power is bounded but may be higher than the peak power of a motor that does not use an elastic element. In the case of the ankle trajectory, for level ground walking at normal speed for an 75 kg subject, the elastic element reduced the peak power of the Maxon motor from 450 W to 132 W. Using the RoboDrive motor the peak power increased depending on the actuator constraints. Future work will extend the proposed methodology in order to reduce peak power of the motor in a SEA.

ACKNOWLEDGMENT

The authors would like to thank Kyle Embry and David Allen for their inspiring discussions on convex optimization and mechanical design of SEAs.

This work was supported by the National Institute of Child Health & Human Development of the NIH under Award Number DP2HD080349. The content is solely the responsibility of the authors and does not necessarily represent the official views of the

NIH. R. D. Gregg holds a Career Award at the Scientific Interface from the Burroughs Wellcome Fund.

REFERENCES

- [1] Albu-Schäffer, A., Eiberger, O., Grebenstein, M., Haddadin, S., Ott, C., Wimbock, T., Wolf, S., and Hirzinger, G., 2008. “Soft robotics”. *IEEE Robot. Autom. Mag.*, **15**(3), pp. 20–30.
- [2] Rouse, E. J., Mooney, L. M., and Herr, H. M., 2014. “Clutchable series-elastic actuator: Implications for prosthetic knee design”. *Int. J. Rob. Res.*, **33**(13), pp. 1611–1625.
- [3] Hollander, K. W., Ilg, R., Sugar, T. G., and Herring, D., 2006. “An Efficient Robotic Tendon for Gait Assistance”. *J. Biomech. Eng.*, **128**(5), p. 788.
- [4] Bolivar, E., Allen, D., Ellson, G., Cossio, J., Voit, W., and Gregg, R., 2016. “Towards a series elastic actuator with electrically modulated stiffness for Powered Ankle-Foot Orthoses”. In *IEEE Int. Conf. Autom. Sci. Eng.*, IEEE, pp. 1086–1093.
- [5] Hurst, J., and Rizzi, A., 2008. “Series compliance for an efficient running gait”. *IEEE Robot. Autom. Mag.*, **15**(3), pp. 42–51.
- [6] Bischoff, R., Kurth, J., Schreiber, G., Koeppe, R., Albu-Schäffer, A., Beyer, A., Eiberger, O., Haddadin, S., Stemmer, A., Grunwald, G., and Others, 2010. “The KUKA-DLR Lightweight Robot arm-a new reference platform for robotics research and manufacturing”. In *Int. Symp. Robot. and German Conf. Robot.*, C. Loughlin, ed., Vol. 34, pp. 1–8.
- [7] Pratt, G., and Williamson, M., 1995. “Series elastic actuators”. In *Proc. 1995 IEEE/RSJ Int. Conf. Intell. Robot. Syst. Hum. Robot Interact. Coop. Robot.*, Vol. 1, IEEE Comput. Soc. Press, pp. 399–406.
- [8] Paine, N., Oh, S., and Sentis, L., 2014. “Design and Control Considerations for High-Performance Series Elastic Actuators”. *IEEE/ASME Trans. Mechatronics*, **19**(3), pp. 1080–1091.
- [9] Hirzinger, G., Sporer, N., Albu-Schäffer, A., Hahnle, M., Krenn, R., Pascucci, A., and Schedl, M., 2002. “DLR’s torque-controlled light weight robot III - are we reaching the technological limits now?”. In *IEEE Int. Conf. Robot. Autom.*, Vol. 2, IEEE, pp. 1710–1716.
- [10] Schutz, S., Mianowski, K., Kotting, C., Nejadfard, A., Reichardt, M., and Berns, K., 2016. “RRLAB SEA A highly integrated compliant actuator with minimised reflected inertia”. In *IEEE Int. Conf. Adv. Intell. Mechatronics*, IEEE, pp. 252–257.
- [11] Robinson, D., Pratt, J., Paluska, D., and Pratt, G., 1999. “Series elastic actuator development for a biomimetic walking robot”. In *IEEE/ASME Int. Conf. Adv. Intell. Mechatronics*, IEEE, pp. 561–568.
- [12] Bicchi, A., and Tonietti, G., 2004. “Fast and “Soft-Arm” Tactics”. *IEEE Robot. Autom. Mag.*, **11**(2), pp. 22–33.
- [13] Braun, D. J., Petit, F., Huber, F., Haddadin, S., van der Smagt, P., Albu-Schäffer, A., and Vijayakumar, S., 2013. “Robots Driven by Compliant Actuators: Optimal Control Under Actuation Constraints”. *IEEE Trans. Robot.*, **29**(5), pp. 1085–1101.
- [14] Vanderborght, B., Verrelst, B., Van Ham, R., Van Damme, M., Lefeber, D., Duran, B. M. Y., and Beyl, P., 2006. “Exploiting Natural Dynamics to Reduce Energy Consumption by Controlling the Compliance of Soft Actuators”. *Int. J. Rob. Res.*, **25**(4), pp. 343–358.
- [15] Jafari, A., Tsagarakis, N. G., and Caldwell, D. G., 2013. “A novel intrinsically energy efficient actuator with adjustable stiffness (AwAS)”. *IEEE/ASME Trans. Mechatronics*, **18**(1), pp. 355–365.
- [16] Williamson, M. M., 1999. “Robot Arm Exploiting Natural Dynamics”. PhD thesis, Massachusetts Institute of Technology.
- [17] Jafari, A., Tsagarakis, N. G., and Caldwell, D. G., 2011. “Exploiting natural dynamics for energy minimization using an Actuator with Adjustable Stiffness (AwAS)”. In *IEEE Int. Conf. Robot. Autom.*, IEEE, pp. 4632–4637.
- [18] Zhao, Y., Paine, N., Kim, K. S., and Sentis, L., 2015. “Stability and Performance Limits of Latency-Prone Distributed Feedback Controllers”. *IEEE Trans. Ind. Electron.*, **62**(11), pp. 7151–7162.
- [19] Knabe, C., Lee, B., Orekhov, V., and Hong, D., 2014. “Design of a Compact, Lightweight, Electromechanical Linear Series Elastic Actuator”. In *Vol. 5B 38th Mech. Robot. Conf.*, ASME.
- [20] Boyd, S., and Vandenberghe, L., 2004. *Convex Optimization*. Cambridge University Press, Cambridge.
- [21] Park, J., and Boyd, S., 2017. “General heuristics for non-convex quadratically constrained quadratic programming”. *arXiv preprint arXiv:1703.07870*.
- [22] Grant, M., and Boyd, S., 2014. CVX: Matlab Software for Disciplined Convex Programming, version 2.1.
- [23] Grant, M. C., and Boyd, S. P., 2008. “Graph Implementations for Nonsmooth Convex Programs”. In *Recent Adv. Learn. Control*, Vol. 371. Springer London, London, pp. 95–110.
- [24] Aps, M., 2017. MOSEK Optimization Suite.
- [25] Quintero, D., Villarreal, D. J., and Gregg, R. D., 2016. “Preliminary experiments with a unified controller for a powered knee-ankle prosthetic leg across walking speeds”. In *IEEE/RSJ Int. Conf. Intell. Robot. Syst.*, IEEE, pp. 5427–5433.
- [26] Winter, D., 1991. *The biomechanics and motor control of human gait: normal, elderly and pathological*, 2nd ed. University of Waterloo Press.
- [27] Jutte, C. V., and Kota, S., 2008. “Design of Nonlinear Springs for Prescribed Load-Displacement Functions”. *J. Mech. Des.*, **130**(8), p. 081403.